

A Self-Powered and Reusable Biocomputing Security Keypad Lock System Based on Biofuel Cells

Ming Zhou,^[a] Xiliang Zheng,^[a] Jin Wang,^{*,[a, b]} and Shaojun Dong^{*,[a]}

Recently, the combination of unconventional chemical logic gates and logic circuits has been used for developing a keypad lock based on an unconventional chemical system,^[1] which is an attractive research direction in the area of unconventional chemical computing and offers a new approach for protecting information.^[2] Such unconventional chemical computing devices can distinguish between the sequences of different chemical inputs.^[1] Despite the promising future for an unconventional chemical keypad lock, there are only a few reports to date and the reported devices are only designed based on luminescent complexes.^[1] In addition to the unconventional chemical keypad lock, the biocomputing keypad lock has been constructed recently.^[3] However, the biocomputing keypad locks are relatively rare and no RESET function was reported,^[3] which would limit their development, especially for practical applications.

Considerable interest has been recently directed towards biofuel cells (BFCs) because of their distinct properties and potential applications, mainly benefiting from the utilization of enzymes^[4] and microbes^[5] as the biocatalysts and biomass as the biofuel to convert chemical energy into electric energy. For instance, the uses of biocatalysts for catalyzing the oxidation of the biofuels essentially enable the BFCs to work under mild conditions, such as ambient temperature and neutral pH.^[4a,b] On the other hand, the uses of biomass, such as glucose, endogenously existing in the biological sys-

tems suggests potential applications of the BFCs as a type of implantable power sources for bioelectronics, including micropumps, pacemakers, and neuromorphic circuits.^[4a] In addition to major research activity relating to long-term operation, miniaturization, and power efficiency of BFCs,^[4] some interesting results were recently reported for BFCs with logically controlled power release by biocomputing.^[6] Biocomputing is a subarea of unconventional chemical computing and ranges from application of biomolecules (proteins, enzymes, and DNA) to the use of whole biological cells for processing biochemical signals in a digital form according to Boolean logic operations.^[3,6,7] Due to the highly specific catalytic or recognition reactions designed by nature, biocomputing can easily solve the interference limitation of chemical computing resulting from the incompatibility in most chemical systems.^[3,6,7]

Herein, we report a novel BFC-based biocomputing security system mimicking a keypad lock device, depending on the enzyme-based parameters as the “readin” and the open circuit potential of the BFC as the “readout”, which permits the biocomputing security system to be self-powered and reusable. By combining BFCs with biocomputing security system, their application might significantly enhance the adaptability of the keypad lock to future self-powered security bioelectronic devices. In addition, we performed a global study and found that maximizing the dimensionless ratio of gap versus standard deviation of the open circuit potential spectrum (a funnel in open-circuit potentials) gives the quantitative optimal design criterion. Thus, our construction reported herein may provide a practical example and microscopic structural basis for mimicking the real biomolecular and network systems and bridge the gaps between the theoretical concepts and experiments important for biomolecular systems and synthetic biology.^[8]

The BFC-based self-powered and reusable biocomputing security system was developed on the basis of a glucose/O₂ BFC reported by us recently with a minor modification (see details in the Supporting Information).^[9] A bioanode formed by the immobilization of glucose dehydrogenase (GDH; E.C. 1.1.3.4, from *Thermoplasma acidophilum*, re-

[a] M. Zhou, X. Zheng, Prof. J. Wang, Prof. S. Dong
State Key Laboratory of Electroanalytical Chemistry
Changchun Institute of Applied Chemistry
Chinese Academy of Sciences
Changchun 130022 (P.R. China)
Fax: (+86) 431-85262101
E-mail: dongsj@ciac.jl.cn

[b] Prof. J. Wang
Department of Chemistry and Department of Physics
State University of New York at Stony Brook
Stony Brook, New York 11794 (USA)
Fax: (+1) 631-6327960
E-mail: jin.wang.1@stonybrook.edu

Supporting information for this article is available on the WWW under <http://dx.doi.org/10.1002/chem.201000619>.

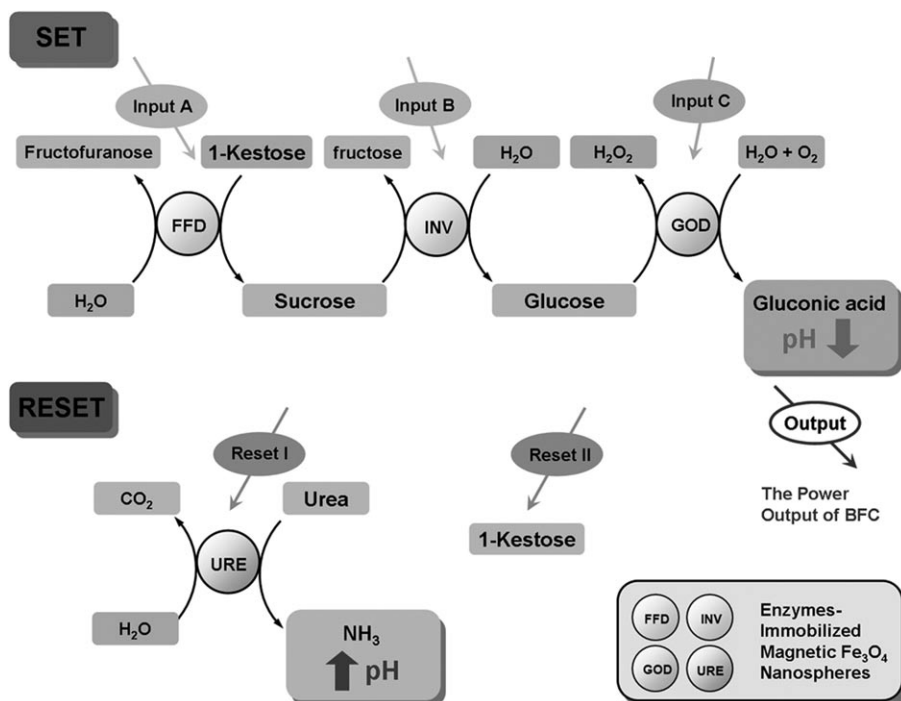
combinant expressed in *Escherichia coli*) exhibited excellent catalytic activity for oxidizing glucose.^[9] On the other hand, the biocathode was immobilized by laccase (LAC; E.C. 1.10.3.2, from *Trametes versicolor*), an enzyme specific for catalyzing a four-electron reduction of O₂.^[9] Compared with the components of the reported BFC,^[9] Nafion 117 film was added as the proton exchange membrane for separating bioanode and -cathode in this work.

Several groups found that LAC bioactivity for O₂ electro-reduction is sensitive to the pH value of the base solution,^[10] which suggests that, in this work, the power output of BFC could be regulated by controlling the pH value of the base solution in the biocathode chamber. In addition, natural biochemical paths include concerted operation of multienzyme systems biocatalyzing chain reactions, which means that taking out one of the biocatalytic units would effectively inhibit the whole chain of the biochemical reactions. Thus, based on the two points above, in the biocathode chamber, we designed a biochemical reaction chain (i.e., hydrolysis of 1-kestose to sucrose, hydrolysis of sucrose to glucose, oxidation of glucose by O₂ to yield gluconic acid) to decrease the pH value and an enzymic catalytic reaction (hydrolysis of urea to NH₃) to increase the pH value for constructing a self-powered and reusable BFC with a keypad lock function (Scheme 1; color version of Scheme 1 is shown in the Supporting Information). These reaction steps were biocatalyzed by FFD (E.C. 3.2.1.80, from *Triticum aestivum*), INV (E.C. 3.2.1.26, from *Saccharomyces cerevisiae*), GOD (E.C. 1.1.3.4, from *Aspergillus niger*), and URE (E.C. 3.5.1.5, from *Canavalia ensiformis* (Jack bean)) immobilized on magnetic

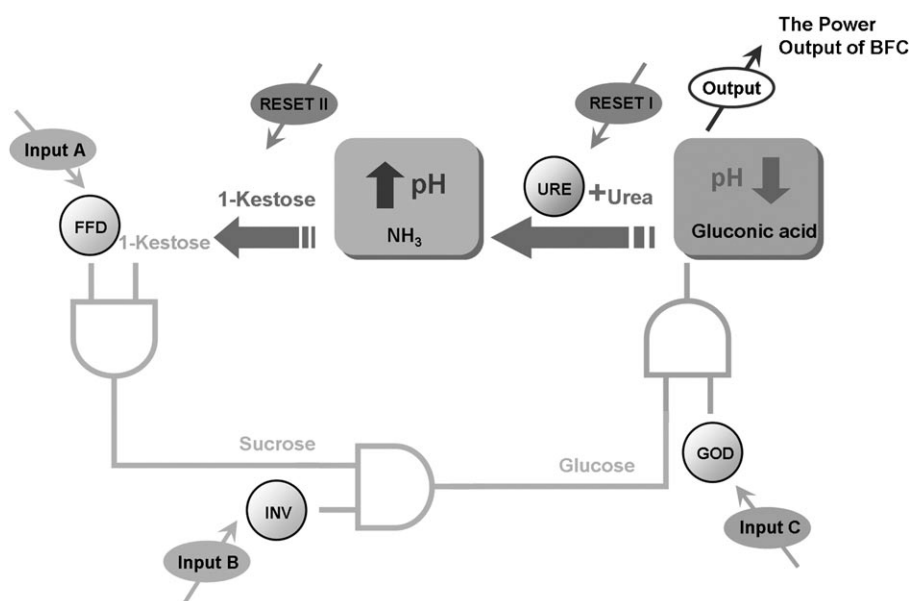
Fe₃O₄ nanospheres (for immobilization details, see the Supporting Information) and they proceeded only in the presence of these enzymes.

The initial system was composed of a bioanode working in 0.1 M pH 6.0 phosphate buffer solution (3 mL) containing 10 mM glucose/20 mM NAD⁺ and a biocathode operating in 0.15 M air-saturated Na₂SO₄ (3 mL) containing 3 mM 1-kestose (both at 37 °C). In the biocathode chamber, the biocatalysts—enzymes (20 mg, FFD, INV, and GOD) immobilized on magnetic Fe₃O₄ nanospheres—served as input signals for the system (A, B, C, respectively) to activate the reaction steps, which can be presented as a network composed of three concatenated AND gates (Scheme 2; color version of Scheme 2 is shown in the Supporting Information). Each AND gate was activated by two input signals: one of them a simple biochemical (1-kestose, sucrose, and glucose) and the second is a biocatalyst FFD, INV, and GOD). The biochemical input signals for the system were considered as 1 when they are present during the reaction time (30 min for each input), and 0 if they are absent. And after the reaction time, enzyme-immobilized magnetic nanospheres were moved away from the biocathode chamber by applying an external magnetic field. We also defined the open-circuit potential of the BFC as output 1, when it was higher than the threshold of 0.4 V and output 0 if it was below 0.4 V. It should be noted that the 1-kestose input signal for the first AND gate was always 1, while sucrose and glucose input signals of 1 for the second and the third AND gates were produced in situ upon the biocatalytic reactions.

In the initial state, the pH value of the base solution in the biocathode chamber (i.e., air-saturated 0.15 M Na₂SO₄ containing 3 mM 1-kestose) was approximately 7.0 [input (0,0,0) in Figure 1A (color version of Figure 1 is shown in the Supporting Information)], in which O₂ reduction at the biocathode was observed at around +0.03 V [input (0,0,0) in Figure 1B). Thus, based on the onset potential of about −0.24 V for glucose oxidation at the bioanode (Anode in Figure 1B), the open-circuit potential of the BFC was approximately 0.27 V [input (0,0,0) in Figure 2 (color version of Figure 2 is shown in the Supporting Information)]. When we set the ABC operation, the chain reactions finally yielded gluconic acid (Scheme 1) resulting in decreasing the pH value from around 7.0 to approximately 4.2 in the biocathode chamber (input (1,1,1) in Fig-



Scheme 1. Biocatalytic reactions in the biocathode chamber of the BFC-based self-powered and reusable bio-computing keypad lock system. FFD = fructan beta-fructosidase, INV = invertase, GOD = glucose oxidase, URE = urease.



Scheme 2. Representation of the BFC-based, self-powered, and reusable biocomputing keypad lock system as a network of three concatenated AND gates and a RESET function.

ure 1 A). Accordingly, the onset potential for O₂ reduction increased clearly (input (1,1,1) in Figure 1 B) and the open-circuit potential of the BFC increased to approximately 0.84 V (input (1,1,1) in Figure 2). This would be attributed to the higher LAC bioactivity for O₂ reduction at a lower pH value (pH < 5) than that in neutral solution in the initial state (pH ≈ 7.0).^[10] The open-circuit potential of the BFC obtained upon eight different patterns of input signals are shown in Figure 2. Based on the concerted operation of multienzyme systems biocatalyzing chain reactions designed by nature, the absence of one of the biocatalytic units would effectively inhibit the whole chain of the biochemical

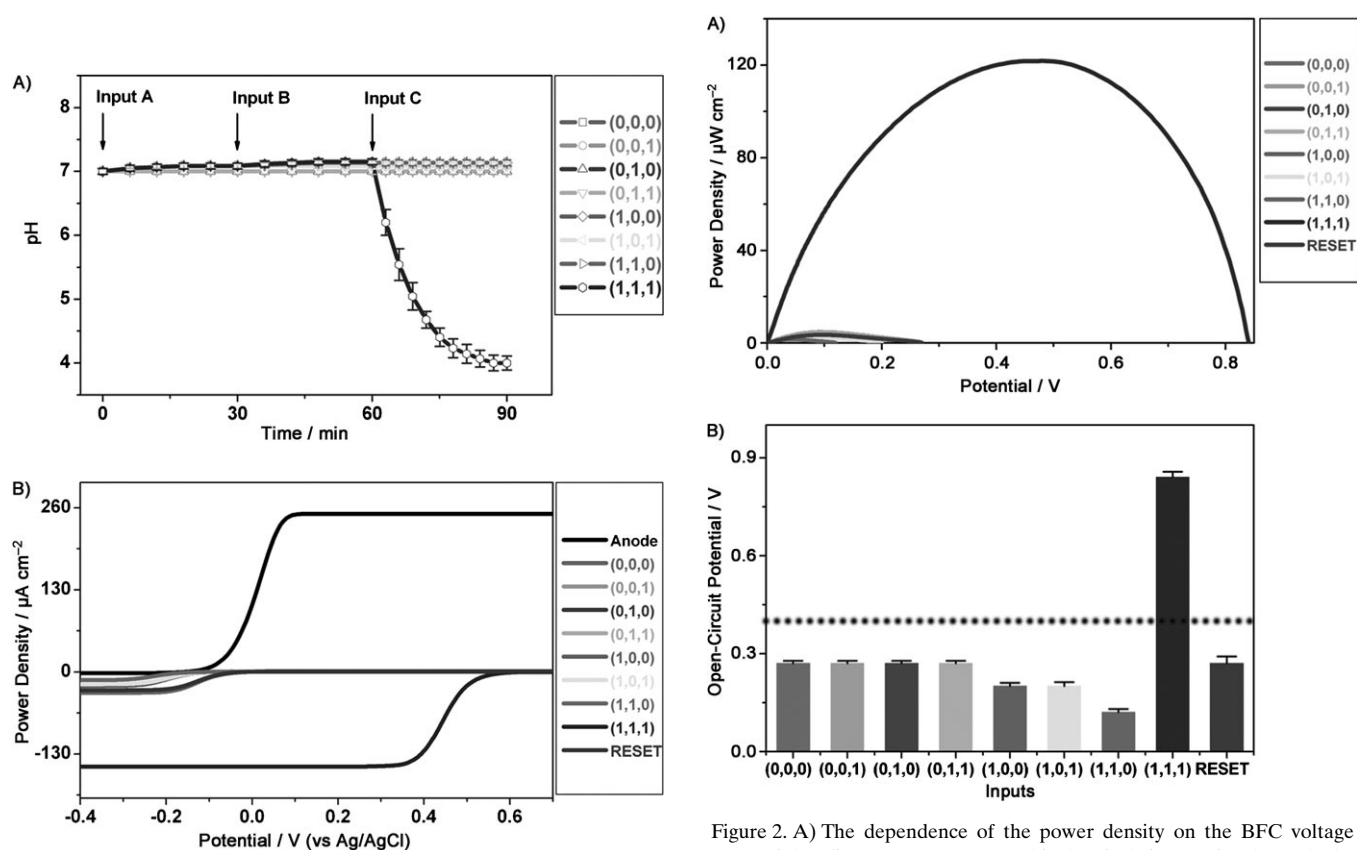


Figure 2. A) The dependence of the power density on the BFC voltage after eight different patterns of biochemical input signals and the RESET function. B) Bar diagram showing the open-circuit potential of the BFC as the output signals generated upon application of eight different patterns of biochemical input signals and the RESET function, suggesting that only one value of the input signals (1,1,1) resulted in the true output signal 1. The dotted line shows the threshold (+0.40 V). The RESET function was operated after input (1,1,1).

Figure 1. A) The pH changes of the base solutions in the biocathode chamber according to Scheme 1 upon the addition of eight different patterns of biochemical input signals. B) Polarization curve of the bioanode and polarization curves of the cathode after eight different patterns of biochemical input signals and the RESET function. Scan rate: 0.1 mV s⁻¹. The RESET function was operated after input (1,1,1).

reactions (Scheme 1). Therefore, the responses obtained from the system correspond to the truth table expected for the sequence of the concatenated AND gates (Scheme 2 and Table S1 in the Supporting Information).

One important feature of the keypad lock system is the dependence of the output signal on the correct order of the input signals. Thus, we performed the experiments when the order of the input signals was varied in six different combinations (Figure 3; color version of Figure 3 is shown in the Supporting Information) and Table S2 in the Supporting Information. Only one correct order of the input signals (ABC) resulted in the true output signal 1, whereas all others produced the false output signal 0. Thus, the developed system represents the IMPLICATION logic operation and the sequence dependence of inputs (i.e., ABC) is mandatory for the construction of BFC-based biocomputing keypad locks.

Another important feature of the present keypad lock system is that it exhibits a RESET function, which makes the system reusable. After completion of the enzyme reactions (i.e., ABC operation), the pH value of base solution (≈ 4.2 , input (1,1,1) in Figure 1A) can be reset to the initial value ($\text{pH} \approx 7.0$, data not shown) by dropping URE-immobi-

lized magnetic Fe_3O_4 nanospheres (20 mg) and urea (6 mM) into biocathode chamber for 30 min (RESET I in Schemes 1 and 2), due to the formation of NH_3 upon hydrolysis of urea biocatalyzed by URE immobilized on magnetic nanospheres. Additionally, after adding 3 mM 1-kestose into the biocathode chamber (RESET II in Schemes 1 and 2), the system was reset to the initial state (RESET in Figures 1B and 2).

To have a global understanding, let us start with a physical analysis of the results obtained (Figure 4). We see that every sequence of operations gives one power output, as shown in

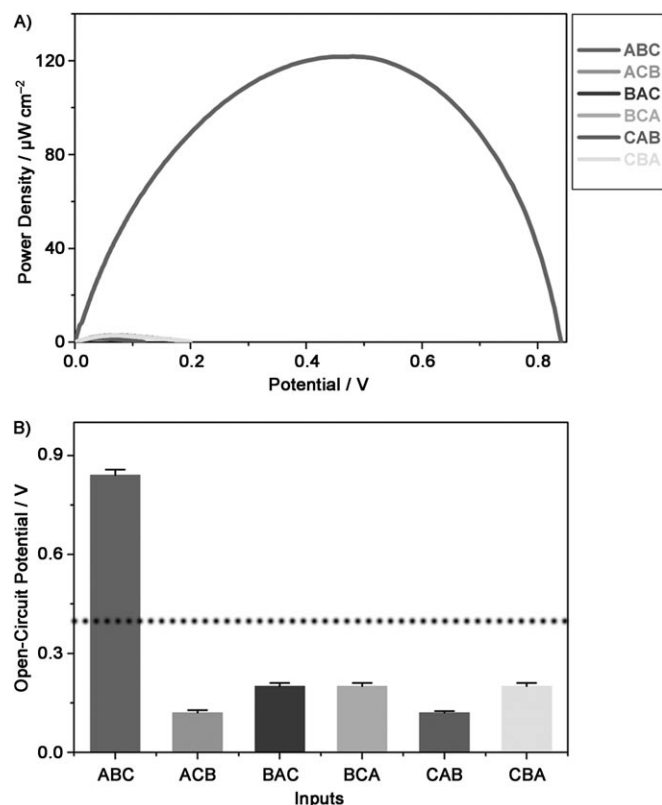


Figure 3. A) The dependence of the power density on the BFC voltage after the input signals 1 were applied in a different order: ABC, ACB, BAC, BCA, CAB, CBA, indicating that only one correct order of the input signals (ABC) resulted in the true output signal 1. B) The bar diagram showing the open-circuit potential of the BFC as the output signals generated upon application of different orders of the input signals. The dotted line shows the threshold (+0.40 V).

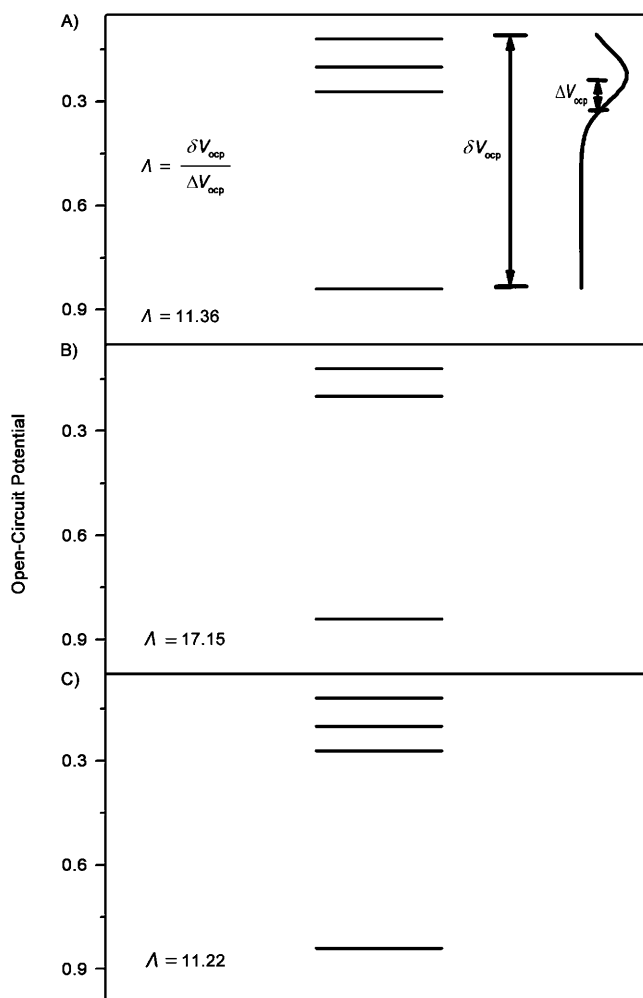


Figure 4. Funneled landscape for the open-circuit potential of the BFC: A) open-circuit potential spectrum for eight different patterns of biochemical input signals, derived from Figure 2 and Table S1; B) open-circuit potential spectrum for six different orders of biochemical input signals, derived from Figure 3 and Table S2; C) open-circuit potential spectrum for eight different patterns of biochemical input signals and six different orders of biochemical input signals, derived from Figure 2 and Table S1 and Figure 3 and Table S2. δV_{ocp} is the gap between the maximum and average open-circuit potential, ΔV is the standard deviation measuring the variance of open-circuit potentials from the mean. The ratio $\Lambda = \delta V_{ocp} / \Delta V_{ocp}$ gives an absolute and dimensionless measure of the degree of funnel and discrimination. The open-circuit potential spectrum forms a funnel-like landscape with a large gap discriminating the best sequence from the others.

Tables S1 and S2 in the Supporting Information. The sequences form an open-circuit potential spectrum. Only the (1,1,1) (equivalent to (ABC)) sequence gives the largest open-circuit potential. The rest of the sequence generates open-circuit potentials less than that of the (1,1,1) sequence. Furthermore, the other open-circuit potentials are significantly less than that of the (1,1,1) sequence. There is a significant gap between the open-circuit potential of the sequence (1,1,1) and that from the rest of the sequences. The discrimination separating the open-circuit potential of sequence (1,1,1) from the rest of the sequences can be clearly seen. The open-circuit potential spectrum here is similar to protein folding and binding energy landscape spectra. In protein folding,^[11] binding,^[12] and signal transduction,^[13] the right sequences of amino acid (or molecules for signal transduction) can form a native functioned state with a significant energy gap separating the native state (or destination for signal transduction) with the rest of the other non-native states. The choice of the right sequences for folding, binding, and signal transduction is from the evolution selection for stable and optimal functions. Here the right sequence of the circuit is selected and designed by us for function (molecular keypad) by the exploration of the sequence space.

As we can see, the sequence of the power outputs forms a funneled landscape with the open-circuit potential of sequence (1,1,1) separated from the rest (Figure 4). To quantify the degree of the discrimination, we introduce two quantities, the gap (δV_{OCP}) and standard deviation (ΔV_{OCP} , square root of variance) of the power output spectrum. The gap, δV_{OCP} , which measures the discrimination, is defined as the difference between the open-circuit potential of the largest sequence ((1,1,1) here) and the average open-circuit potentials of the rest of the sequences. The standard deviation, ΔV_{OCP} , which measures the dispersion, is the square root of the variance of the open-circuit potentials of the rest of the sequences. The ratio $\mathcal{A} = \delta V_{\text{OCP}} / \Delta V_{\text{OCP}}$ gives an absolute and dimensionless measure of the degree of funnel and discrimination. When \mathcal{A} is large (significantly larger than one), the landscape or spectrum of the open-circuit potential has a large gap relative to the variations of other sequences, which effectively separates the (1,1,1) sequence from the rest of the sequences. This forms an effective funneled landscape of power output towards the (1,1,1) sequence. Therefore, we can see that, physically, a funneled landscape towards the selected sequence quantified by the ratio $\mathcal{A} = \delta V_{\text{OCP}} / \Delta V_{\text{OCP}}$ provides an optimal design criterion for discrimination of open-circuit potentials for molecular keypad function. Details are given in Figure 4 and Table S3 in the Supporting Information.

In conclusion, we have demonstrated a novel biocomputing security system based on a self-powered and reusable BFC mimicking a keypad lock device. Coupling BFCs with keypad locks might not only significantly increase the versatility of BFCs resulting in the BFC-based biocomputing security system, but also greatly enhance the adaptability of the keypad lock to future self-powered and reusable biocomputing security system based bioelectronic devices. The

study may also shed light on mimicking and designing natural signal transduction, metabolic, and gene regulation systems.^[8] One can think of the example shown in Scheme 1 as composed of three motifs. The three inputs act as connectors to the reaction modules, so that the three reactions can cascade down normally to produce the positive output responses. This system is analogous to a signal transduction subnetwork MAP Kinase with three motifs of enzyme reactions of phosphorylation–dephosphorylation connected together.^[13] These motifs mimic the logic gates. The function of MAP Kinase subnetwork is to transmit the information flow from up- to downstream in a fast and reliable way. The specific sequence combination of the MAP Kinase motif generates the overall funneled landscape,^[13] which guarantees the unique direction of information flow and stability of the function. Herein, we constructed a system to perform logic gate functions. Only with specific sequences of three AND gates, it can guarantee the resulting functions, therefore, effectively generates an overall funneled landscape. The system with other combinations of sequences will effectively generate a rough landscape and will not guarantee the required function. Our approach provides a new way of mimicking the biological systems and is therefore important for designing systems and synthetic biology.^[8] It also bridges the gap between theoretical concepts, such as information/landscape theory and experiments as well as practical realizations of chemical and biological systems.

Experimental Section

For full details, see the Supporting Information.

Acknowledgements

S.D. would like to thank the National Natural Science Foundation of China (nos. 20935003 and 20820102037) and 973 Project (nos. 2009CB930100 and 2010CB933600) for support. J.W. would like to thank the National Science Foundation for support.

Keywords: biocomputing • biofuel cells • enzymes • molecular electronics • self-powered systems

- [1] a) D. Margulies, C. E. Felder, G. Melman, A. Shanzer, *J. Am. Chem. Soc.* **2007**, *129*, 347–354; b) M. Suresh, A. Ghosh, A. Das, *Chem. Commun.* **2008**, 3906; c) W. Sun, C. Zhou, C. H. Xu, C. J. Fang, C. Zhang, Z. X. Li, C. H. Yan, *Chem. Eur. J.* **2008**, *14*, 6342–6351; d) M. Kumar, A. Dhir, V. Bhalla, *Org. Lett.* **2009**, *11*, 2567–2570; e) J. Andréasson, S. D. Straight, T. A. Moore, A. L. Moore, D. Gust, *Chem. Eur. J.* **2009**, *15*, 3936–3939; f) S. Kumar, V. Luxami, R. Saini, D. Kaur, *Chem. Commun.* **2009**, 3044–3046; g) M. Kumar, R. Kumar, V. Bhalla, *Chem. Commun.* **2009**, 7384–7386.
- [2] a) P. A. de Silva, N. H. Q. Gunaratne, C. P. McCoy, *Nature* **1993**, *364*, 42–44; b) K. L. Kompa, R. D. Levine, *Proc. Natl. Acad. Sci. USA* **2001**, *98*, 410–414; c) F. Remacle, E. W. Schlag, H. Selzle, K. L. Kompa, U. Even, R. D. Levine, *Proc. Natl. Acad. Sci. USA* **2001**, *98*,

- 2973–2978; d) K. Szacilowski, W. Macyk, G. Stochel, *J. Am. Chem. Soc.* **2006**, *128*, 4550–4551.
- [3] a) G. Strack, M. Ornatska, M. Pita, E. Katz, *J. Am. Chem. Soc.* **2008**, *130*, 4234–4235; b) J. Hala'mek, T. K. Tam, S. Chinnapareddy, V. Bocharova, E. Katz, *J. Phys. Chem. Lett.* **2010**, *1*, 973–977.
- [4] a) S. C. Barton, J. Gallaway, P. Atanassov, *Chem. Rev.* **2004**, *104*, 4867–4886; b) A. Heller, *Anal. Bioanal. Chem.* **2006**, *385*, 469–473; c) J. A. Cracknell, K. A. Vincent, F. A. Armstrong, *Chem. Rev.* **2008**, *108*, 2439–2461; d) M. J. Moehlenbrock, S. D. Minter, *Chem. Soc. Rev.* **2008**, *37*, 1188–1196.
- [5] B. E. Logan, B. Hamelers, R. Rozendal, U. Schroder, J. Keller, S. Freguia, P. Aelterman, W. Verstraete, K. Rabaey, *Environ. Sci. Technol.* **2006**, *40*, 5181–5192.
- [6] a) L. Amir, T. K. Tam, M. Pita, M. M. Meijler, L. Alfonsa, E. Katz, *J. Am. Chem. Soc.* **2009**, *131*, 826–832; b) T. K. Tam, G. Strack, M. Pita, E. Katz, *J. Am. Chem. Soc.* **2009**, *131*, 11670–11671; c) M. Zhou, Y. Du, C. Chen, B. Li, D. Wen, S. Dong, E. Wang, *J. Am. Chem. Soc.* **2010**, *132*, 2172–2174.
- [7] a) M. N. Stojanovic, D. Stefanovic, *J. Am. Chem. Soc.* **2003**, *125*, 6673–6676; b) A. Saghatelian, N. H. Volcker, K. M. Guckian, V. S. Y. Lin, M. R. Ghadiri, *J. Am. Chem. Soc.* **2003**, *125*, 346–347; c) D. M. Kolpashchikov, M. N. Stojanovic, *J. Am. Chem. Soc.* **2005**, *127*, 11348–11351; d) T. Niazov, R. Baron, E. Katz, O. Lioubashevski, I. Willner, *Proc. Natl. Acad. Sci. USA* **2006**, *103*, 17160–17163; e) S. Muramatsu, K. Kinbara, H. Taguchi, N. Ishii, T. Aida, *J. Am. Chem. Soc.* **2006**, *128*, 3764–3769.
- [8] a) E. H. Davidson, D. H. Erwin, *Science* **2006**, *311*, 796–797; b) N. E. Buchler, U. Gerland, T. Hwa, *Proc. Natl. Acad. Sci. USA* **2003**, *100*, 5136–5141.
- [9] M. Zhou, L. Deng, D. Wen, L. Shang, L. Jin, S. Dong, *Biosens. Bioelectron.* **2009**, *24*, 2904–2908.
- [10] a) Y. Liu, M. Wang, F. Zhao, B. Liu, S. Dong, *Chem. Eur. J.* **2005**, *11*, 4970–4974; b) N. Mano, H.-H. Kim, Y. Zhang, A. Heller, *J. Am. Chem. Soc.* **2002**, *124*, 6480–6486; c) F. Xu, *Biochemistry* **1996**, *35*, 7608–7614.
- [11] P. G. Wolynes, J. N. Onuchic, D. Thirumalai, *Science* **1995**, *267*, 1619–1620.
- [12] a) J. Wang, G. M. Verkhivker, *Phys. Rev. Lett.* **2003**, *90*, 188101/188101–188104; b) J. Wang, X. Zheng, Y. Yang, D. Drueckhammer, W. Yang, G. Verkhivker, E. Wang, *Phys. Rev. Lett.* **2007**, *99*, 198101/198101–198104.
- [13] a) J. Wang, B. Huang, X. Xia, Z. Sun, *Biophys. J.* **2006**, *91*, L54 L56; b) J. Wang, K. Zhang, E. Wang, *J. Chem. Phys.* **2008**, *129*, 135101–135109.

Received: March 10, 2010

Published online: May 28, 2010